Heugenhauser *et al.*
Acta Neuropathologica Communications (2024) 12:183
https://doi.org/10.1186/s40478-024-01888-8

Acta Neuropathologica Communications

RESEARCH

Open Access

Towards integrating imaging and immunology in glioblastoma: mapping blood immune system metrics to tumor magnetic resonance image data

Johanna Heugenhauser[1], Carmen Visus[2], Johanna Buchroithner[3], Christine Marosi[4], Karl Rössler[5], Thomas Felzmann[6], Georg Widhalm[5], Sarah Iglseder[1], Martha Nowosielski[1] and Friedrich Erhart[5*]

Abstract

Background Glioblastoma is the most frequent and aggressive brain cancer. It is a highly immunology-driven disease as up to a third of its mass is composed of immune cells. Apart from immunology, imaging is a major research frontier. The VASARI (Visually AcceSAble Rembrandt Images) MRI feature set is a system designed to enable consistent description of gliomas using a set of defined visual features and controlled vocabulary. Even though imaging and immunology are both indispensable for glioblastoma phenotyping, a comprehensive integration of these two disciplines has not been performed so far.

Material and methods 76 patients from a previous glioblastoma immunotherapy clinical trial were retrospectively screened for the availability of peripheral blood immunology and tumor imaging data at baseline, i.e. at the start of the study. For 41 patients both were available. MRI were then analyzed via volumetry and VASARI morphometry. The resulting 27 imaging variables were linked with 67 peripheral blood immunology variables from flow cytometry and PCR and all potential relations were mapped.

Results In an initial broad screening, 94 imaging-immunology associations were discovered. Notably, features of the contrast-enhancing margin like its thickness and its shape were positively correlated with various T cell species including activated cytotoxic CD8+ T cells and central memory CD8+ T cells. The T2-volume was correlated with CD56+CD16− natural killer cells, and the necrosis volume was correlated with immunopolarizing mRNAs in the blood (IFN-γ, GATA3, ROR-gt). After multiple testing correction, two imaging-immunology associations were confirmed as significant: a thick contrast-enhancing margin was correlated with lower regulatory T cell markers in the blood and invasion of deep white matter was correlated with less T helper 17 factors.

Conclusion We here provide first evidence that imaging and peripheral blood immunology features can go hand in hand and that imaging variables can correlate with systemic immunophenotypes. Especially a thick contrast-enhancing margin seems to indicate a pro-inflammatory immune state. Via pioneering the integration of imaging and immunology, we not only advance basic glioblastoma science but we also open up novel avenues

Originality and Presentations: The authors confirm the originality of this study.

*Correspondence:
Friedrich Erhart
friedrich.erhart@meduniwien.ac.at
Full list of author information is available at the end of the article

for research. In the future, e.g. patient stratification for therapy development could be based on imaging-guided immunophenotyping.

Keywords Glioblastoma, Immunology, Magnetic resonance imaging, Volumetry, VASARI

Introduction

Glioblastoma is the most frequent and most aggressive primary brain tumor [29]. Novel approaches to understanding and treating it are desperately needed. Currently, a major research frontier in glioblastoma is immunology [27], also because a substantial part of glioblastoma's cell mass—by some accounts up to a third—is composed of immune cells [19, 24]. In line with that, all aspects of glioblastoma treatment research are touched by the immune system: innovative immunotherapies being developed are intimately dependent on the specific immunology found within the tumor [20]. Likewise, established treatment modalities have to take the immune system into account. Chemotherapy with temozolomide has multiple and complex effects, ranging from enhanced T cell proliferation after initial lymphopenia to altered dendritic cell function [6, 17]. And radiotherapy can induce immunogenic cell death and potent immune-stimulation [25]. Importantly, even before treatment, i.e. at baseline, the tumor already heavily interacts with the immune system and conditions it [15]. Apart from local immunosuppression, also systemic immunological dynamics are triggered at baseline, e.g. driven by the altered blood–brain-barrier [20]. This aspect, the baseline systemic immunology, is at present less well established than immunological changes upon treatment. One major axis where baseline immunology could be explored deeper is in conjunction with tumor morphology as it is currently not known in how far certain morphology features condition the immune system. But it could well be that specific imaging aspects go hand in hand with specific immune system phenotypes. A hitherto hardly explored approach could be harnessing existing imaging data to elucidate possible immunology-imaging-connections.

Aptly, the analysis of tumor morphology, structure and architecture via imaging is a second major frontier in glioblastoma research. MRI is the gold standard e.g. for surgery and radiotherapy planning. Of the imaging interpretation protocols available, especially the VASARI (Visually AcceSAble Rembrandt Images) approach has proven to be of great utility and is widely used [1, 16, 22, 28]. The VASARI MRI feature set is a system designed to enable consistent description of gliomas using a set of defined 24 visual features and controlled vocabulary e.g. tumor location, deep white matter invasion and morphological classification of the contrast-enhancing tumor margin. Volumetry and VASARI have been applied to a plethora of research questions, but in direct connection with systemic immunology data they have so far hardly been investigated.

In fact, the two fields of glioblastoma immunology and glioblastoma radiology are kept surprisingly separate given that glioblastoma is an immunology-driven disease. Combining baseline immunology and imaging could pave the way for a more comprehensive understanding of glioblastoma. And, better characterizing the initial state of the immune system by means of imaging would not only be relevant from a fundamental, basic research point of view but could also be clinically useful. It may aid in stratifying patients and personalizing therapies—even enabling immunology-based precision medicine. Thus, with the present work we aim at closing the currently existing gap. We combine baseline peripheral blood immunology data from a previous clinical study with a comprehensive imaging analysis including structured morphology measurement with volumetry and VASARI. In doing so, we aim to discover hitherto unknown connections between imaging features and systemic immune features.

Methods

Patients

All patients retrospectively analyzed in this study had been enrolled in a nation-wide, randomized, multicenter, open-label phase II glioblastoma dendritic-cell vaccine (Audencel) trial with EudraCT number 2009-015979-27 [3]. Each patient was suffering from a newly diagnosed glioblastoma WHO grade IV, according to the 2016 World Health Organization Classification of Tumors of the Central Nervous System [21]. All patients had given written informed consent before trial entry. The study had been reviewed and approved by the local independent ethics committee and institutional review board (number TRX 2/P-II-018).

Variable characteristics

A total of 94 variables were investigated—27 radiological and 67 immunological. The 27 radiological variables arise from four different kinds of newly performed tumor characterization on baseline MRI: 3 standard volumetry features (the contrast enhancing tumor region depicted in T1 contrast enhancing sequences, the necrotic core and the T2 hyperintense tumor volume, i.e. a mixture of edema,

infiltrating tumor and immune cells seen as a T2 hyperintense signal), as well as according to the VASARI MRI feature set system that comprises 24 unique morphological tumor features. The 67 immunological variables were measured as part of the original immunotherapy trial. They were based on flow cytometric characterization of peripheral blood immune cell populations as well as PCR of immunophenotype-related factors measured in peripheral blood immune cells—from blood taken at baseline of the clinical trial, several days after imaging, before study-specific interventions and before brain tumor excision surgery. The only minor exception are the 5 "elutra" variables that were measured after surgery (see below).

Immunological data

The exact immunological methods applied to peripheral blood from each patient have previously been described in detail [7]. Briefly, blood immune cell populations at baseline were analyzed via flow cytometry of surface markers on a BD LSR-II cytometer (BD Bioscience, Heidelberg, Germany). Polarization towards a T helper 1 (Th1), T helper 2 (Th2), T helper 17 (Th17) or regulatory T cell (Treg) phenotype was measured via qRT-PCR of characteristic factors (IFNγ, TBET, IL4, GATA3, IL10, FOXP3, TGFβ, IL17A, RORγT) via the Taqman® 7500 Violet PCR system (Applied Biosystems). Additionally, surface markers were also measured when blood cells were separated via elutriation with the Elutra system for cell therapy production purposes [2], which was performed after brain tumor removal surgery. The respective variables are denoted with "elutra".

Magnetic resonance imaging acquisition

Owing to the multicenter design of the original trial, multiple MRI systems were used, all operating at a 1.5T field strength. A 3D T1-weighted imaging protocol including magnetization-prepared rapid acquisition with gradient echo (MP-RAGE) MRI sequences or T1-weighted spin-echo (SE) images with contrast enhancement (0.1 mmol/kg gadopentetate dimeg-lumine) was performed at each center, resulting in images of similar resolution, with a slice thickness of at least 1.5 mm. All patients underwent axial T2- or FLAIR-weighted imaging with a slice thickness of at least 2 mm. In this study we only analyzed baseline MRI, carried out before surgery/ radiation/ systemic therapy.

Segmentation and volumetry on MRI

Contrast-enhanced lesions in T1-weighted images (excluding dura, blood vessels, the resection cavity and/or central necrotic area), central necrotic area in T1-weighted images, and hyperintense T2/FLAIR lesions (excluding the contrast enhanced and necrotic tumor portions) were segmented and volumes were calculated using a semi-automated active contour method (ITK-SNAP 3.4.0; www.itksnap.org [34]) called "snake evolution". "Snake" is a 3D description of a closed curve or surface that represents a segmentation. It starts as an estimate of the anatomical structure of interest and continues to a close approximation of the structure. Evolution of the "snake" is governed by a mathematical equation describing the velocity of every point on the "snake" at any particular time. This segmentation tool demonstrated excellent reliability and high efficiency of 3D segmentation and it has already been used in various projects for tumor volumetry [10, 34].

VASARI

24 semantic descriptors of imaging features from VASARI based on the baseline MRI were extracted. Those features were seven ordinal, thirteen binary, five categorical and three continuous variables. In order to confirm that VASARI features are a valid method for assessing semantic imaging descriptors in this study, two independent raters (H.J. and I.S.) performed the analysis of VASARI features of all patients. A summary of all extracted VASARI features is given in Supplementary Table 1. A detailed description of the VASARI features can be found on The Cancer Imaging Archive VASARI research project webpage: (https://wiki.cancerimagingarchive.net/display/Public/VASARI+Research+Project) [16].

Statistical analysis

Statistical analyses were performed using R software version 4.2.1, IBM SPSS Statistics Version 29.0.0.0 and GraphPad Prism version 9.5.0. For retrospective power analysis G*Power version 3.1.9.3 was used. P-values less than 0.05 were considered significant.

To calculate the inter-rater reliabity between two independent raters, Cohen's kappa was calculated. Pearson's analysis was used for correlations between quantitative immunologic parameters and quantitative VASARI features (with a normal distribution). Spearman test was used for correlations between quantitative immunologic parameters and ordinal, i.e. also semiquantitative, VASARI features. Point-biserial correlation was used for correlations between quantitative immunological parameters and binary VASARI features. After an initial broad screening for exploratory purposes, all results of correlation analyses were corrected for multiple comparison (Bonferroni's adjustment). Differences among categorical/binary VASARI features and quantitative immunologic parameters were evaluated with one-way ANOVA

followed by Tukey test. Cohen's f value was calculated for the power analysis, which was a retrospective power analysis where a sample size of 76 and a significance level of 0.05 (alpha) were used. As effect size, the correlation coefficients for correlation analysis, and Cohen's f for one-way ANOVA tests were used.

For unsupervised, data-driven discovery of patterns in the multidimensional variable space, k-means clustering, principal component analysis (PCA) and t-distributed stochastic neighbor embedding (t-SNE) were performed. Clustering calculation and graphical represention as a heatmap were performed with the ComplexHeatmap package in R [9]. The PCA plot was calculated and generated with the ggfortiy packacke in R [11, 31]. The t-SNE computation was performed with the Rtsne package [18, 32, 33].

Table 1 Patient characteristics at baseline

Number of patients		**41**
Sex, n (%)	Male	25 (61.0)
	Female	16 (39.0)
Median age at diagnosis, years (95% CI)		56.6 (52.7–60.6)
Median overall survival, months (95% CI)		21.0 (16.7–25.2)
ECOG at baseline, n (%)	0	14 (34.1)
	1	27 (65.9)
MGMT promoter, n (%)	Samples measured	37 (90.2)
	Methylated	13/37 (35.1)
	Unmethylated	24/37 (64.9)
IDH 1 mutation, n (%)	Wildtype	41 (100)
Side of tumor bulk, n (%)	Left	17 (41.5)
	Right	22 (53.7)
Tumor location, n (%)	Central/bitemporal	2 (4.9)
	Frontal	14 (34.1)
	Temporal	5 (12.2)
	Parietal	9 (22.0)
	Occipital	13 (31.7)

n: number of patients, ECOG: Eastern Cooperative Oncology Group, MGMT: O-6-methylguanine-DNA methyltransferase, IDH: isocitrate dehydrogenase 1

Results

Patient characteristics

All 76 patients from the cohort were screened for radiological and immunological data. Radiological data was available for 76 patients and immunological data for 49 patients, both types of measurement were available for 41 patients. The resulting cohort of 41 patients under investigation comprised 25 men and 16 women. The median age at tumor diagnosis was 56.6 years. All patients had glioblastoma as the histological diagnosis (as per the original pathological report) and for all patients the IDH status was wild-type. Table 1 gives an overview of further main patient characteristics.

General description of imaging data

The median tumor volume across all patients studied was 21.7 cm^3, the median volume of the necrotic core was 14.2 cm^3 and the median T2 hyperintense volume was 55.6 cm^3. Further key observations according to the VASARI framework were e.g. that frontal was the most frequent tumor location and that the majority of tumors showed an infiltrative growth pattern. All further measurements are listed in Supplementary Table 1. The inter-observer reliability between the two independent raters of all VASARI features was excellent ($\mathfrak{R} = 0.925$).

Mapping of correlations between quantitative imaging and immunology variables

As first main analysis, potential associations between quantitative imaging (22 in total) and immune variables were mapped. For that, a full correlation matrix (Fig. 1) was calculated that gives a complete overview of all imaging and immune connections. We could observe that 94 out of all 1474 potential variable pairs showed a statistically significant correlation—at that stage without multiple testing correction as the first goal was an exploratory, comprehensive screening. Of the 94 associations, 41 were a positive correlation and 53 a negative correlation. The variable pairs with the strongest statistically significant positive correlation were "T2 volume"/"CD56+CD16− cells" ($r = 0.6$, $p < 0.001$), "definition of enhancing margin"/"activated CD8+ cells" ($r = 0.5$, $p < 0.001$) and

(See figure on next page.)

Fig. 1 Correlation matrix between quantitative imaging and immunology variables. The respective r values of significant correlations are depicted. Only r values with a significant *p*-value ($p < 0.05$) are shown. Each r value is colored according to a specific value (e.g. an r value of −0.4 is colored in light green). The reference colors of each value can be seen on the right side of the figure. They are based on the respectively appropriate statistical correlation test depending on the nature of the variable pair (see Methods) and cover all variable types apart from categorical imaging variables (where no correlation can be calculated from a statistical point of view and which are thus analyzed in the subsequent section). CD: cluster of differentiation, neg: negative, EM: effector memory, dif: differentiated, CM: central memory, NKT: natural killer T cells, Tregs: regulatory T cells, Th: T helper cells, HLA-DR: human leukocyte antigen-DR isotype, MDSC: myeloid-derived suppressor cells, IFNg: interferon gamma, mRNA: messenger ribonucleic acid, PBMC: peripheral blood mononuclear cell, IL: interleukin, ROR-gt: RAR-related orphan receptor gamma, FOXp3: forkhead box P3, TGFb: transforming growth factor beta, CET: contrast enhancing tumor, nCET: non-contrast enhancing tumor, FLAIR: fluid attenuated inversion recovery

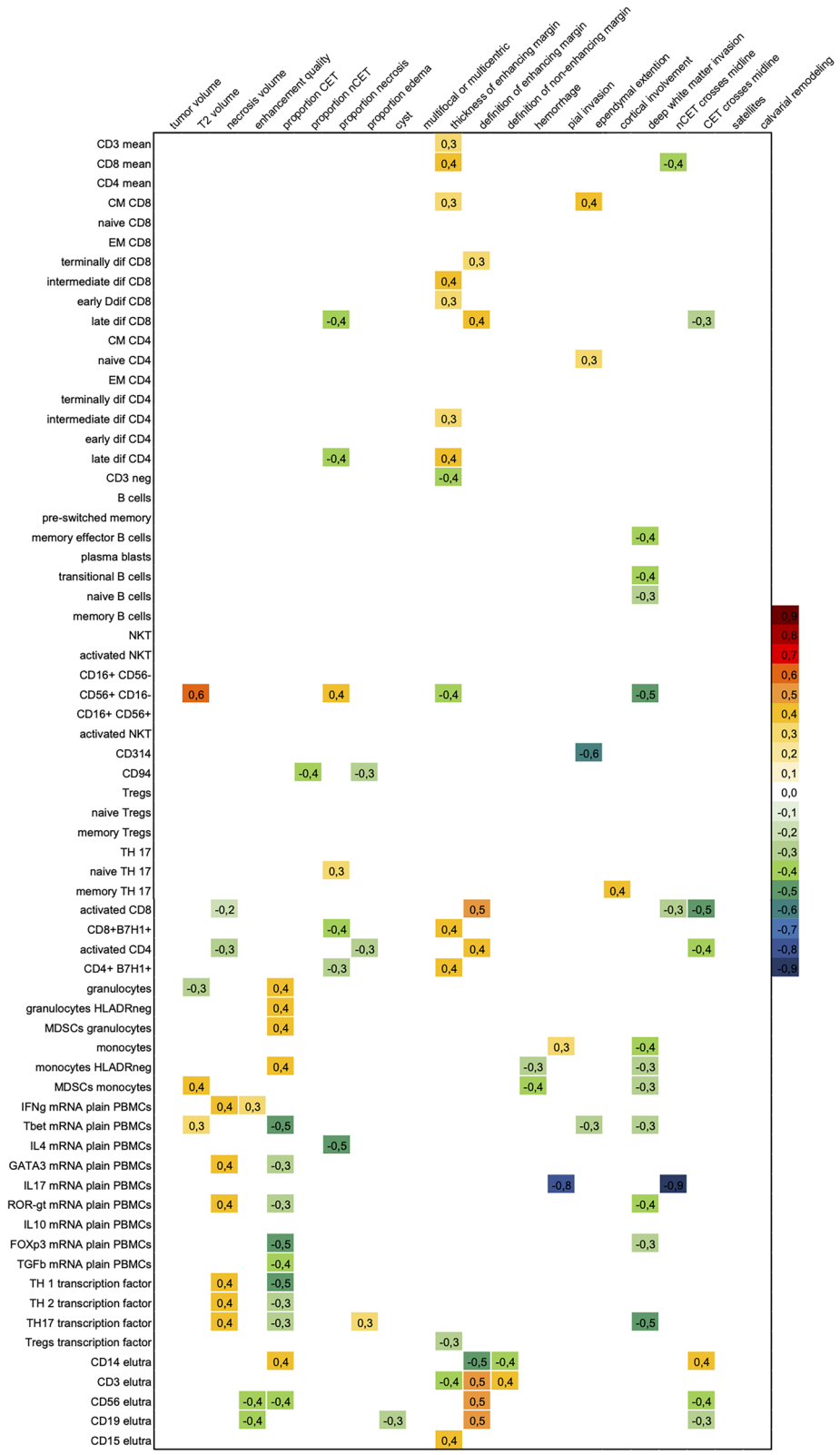

Fig. 1 (See legend on previous page.)

"definition of enhancing margin"/"CD3 elutra" (r = 0.5, $p = 0.001$), "definition of enhancing margin"/"CD56 elutra" (r = 0.5, $p < 0.001$) and "definition of enhancing margin"/"CD19 elutra" (r = 0.5, $p = 0.003$). This means that the T2 volume of the glioblastoma was correlated with the number of CD56+CD16− natural killer (NK) cells in the peripheral blood as measured by flow cytometry (Fig. 2). Further, it means that a well-defined contrast-enhancing margin on MRI, hence its shape, was associated with the number of activated CD8+ cytotoxic T cells in the blood. The same holds true for CD3+ T cells overall, CD56+NK cells and CD19+ B cells (as measured after elutriation, see Methods) that were also associated with a well-defined contrast-enhancing margin. A further, additional notable observation in terms of positive correlations (see Fig. 1) was that the "thickness of the enhancing margin" was associated with many immune variables, among them e.g. "central memory CD8+" (r = 0.3, $p = 0.039$, Fig. 3), "CD8+ mean" (r = 0.4, $p = 0.012$), and "intermediate differentiated CD8+" (r = 0.4, $p = 0.013$), i.e. several cytotoxic T cell-related variables. What is more, the "necrosis volume" showed a positive correlation with several blood mRNAs, namely interferon gamma (IFN-γ, an immunostimulatory, T helper 1 promoting cytokine, r = 0.4, $p = 0.024$, Fig. 4), GATA3 (an immunostimulatory, T helper 2 promoting transcription factor, r = 0.4, $p = 0.024$) and ROR-gt (a T helper 17 promoting transcription factor, r = 0.4, $p = 0.013$). When examining pairs of imaging and immunology variables with a negative correlation, three of them showed a notably strong association. Interleukin-17 (IL-17) mRNA in the blood was negatively correlated with midline-crossing of the non-contrast enhancing tumor part (variable "nCET crosses midline", i.e. the FLAIR/T2 extension) (r = −0.9, $p < 0.001$) and with pial invasion (r = −0.8, $p = 0.016$). Ependymal extension of the tumor was negatively correlated with CD314+ (NKG2D) cells in the blood, i.e. NK cells (r = −0.6, $p < 0.001$). Summing up, the most prominent observation of the screening was that multiple features of the contrast-enhancing margin are associated with pro-inflammatory cytotoxic T cell species.

Mapping of connections between categorical imaging and immunology variables

For categorical variables (5 in total, e.g. "side of the tumor"), correlation computation is not adequate but associations can be mapped via ANOVA testing. Supplementary Fig. 1 represents a respective association matrix similar to the one used above—again as a comprehensive screening without advanced multiple testing correction. Here, 4 out of 335 imaging and immunology variable pairs showed a significant finding (Fig. 5): (A) Terminally differentiated CD4+ helper T cells in the blood were higher in central/bilateral tumors than in left- or right-sided tumors (bilateral-left, $p = 0.078$; bilateral-right, $p = 0.041$). (B) On the contrary, peripheral blood monocytes were lower in central/bilateral tumors than in left- or right-sided tumors (bilateral-left, $p = 0.283$;

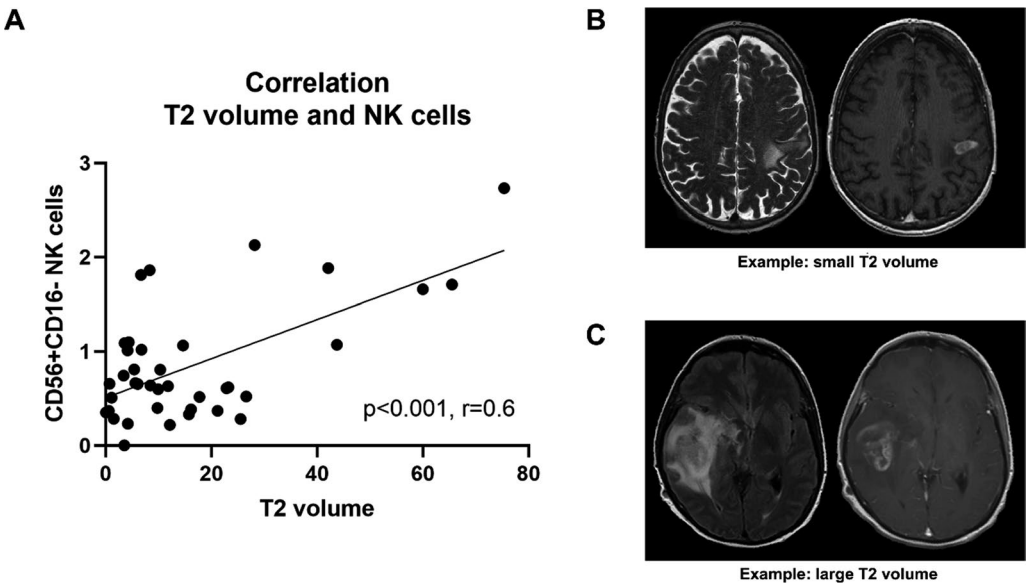

Fig. 2 T2 hyperintense volume and CD56+CD16− NK cells in the blood. Tumor T2 volume correlated significantly with the abundance of CD56+CD16− NK cells in the peripheral blood (**a**), measured via Pearson correlation. As illustration, an example of a patient with a relatively small T2 volume (**b**) and a patient with a relatively large T2 volume (**c**) are given

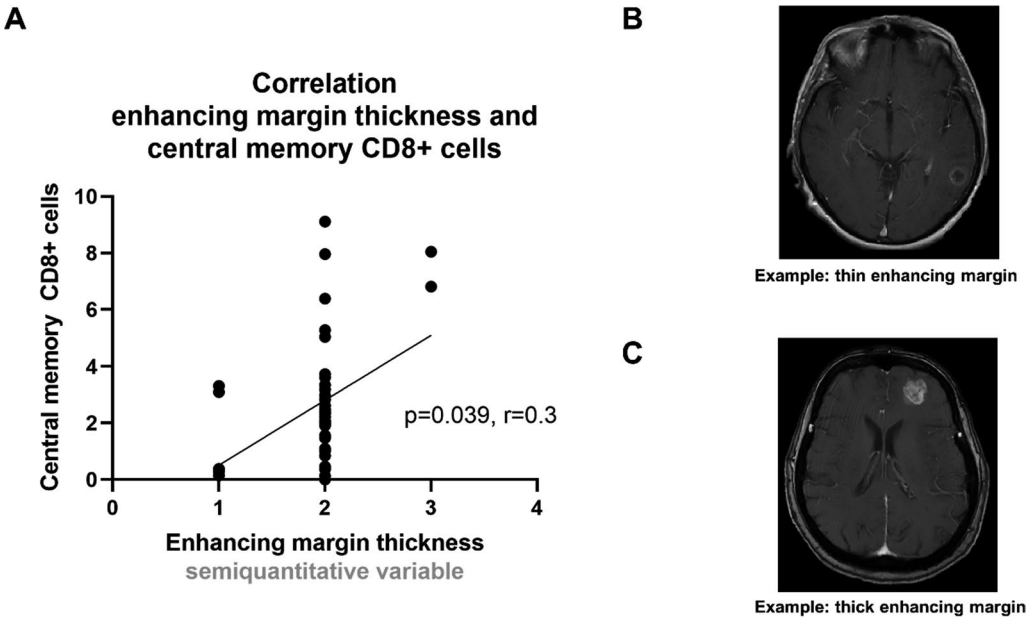

Fig. 3 Enhancing margin thickness and central memory CD8+ cells in the blood. The thickness of the enhancing margin (which is assessed semiquantitatively as an ordinal variable in the VASARI methodology: 1 = thin, 2 = thick, 3 = solid) correlated significantly with the abundance of central memory CD8+ cells in the peripheral blood (**a**), as measured via Spearman correlation that is the adequate test for correlating semiquantitative/ordinal variables with quantitative variables. As illustration, an example of a patient with a relatively thin enhancing margin (**b**) and a patient with a relatively thick enhancing margin (**c**) are given

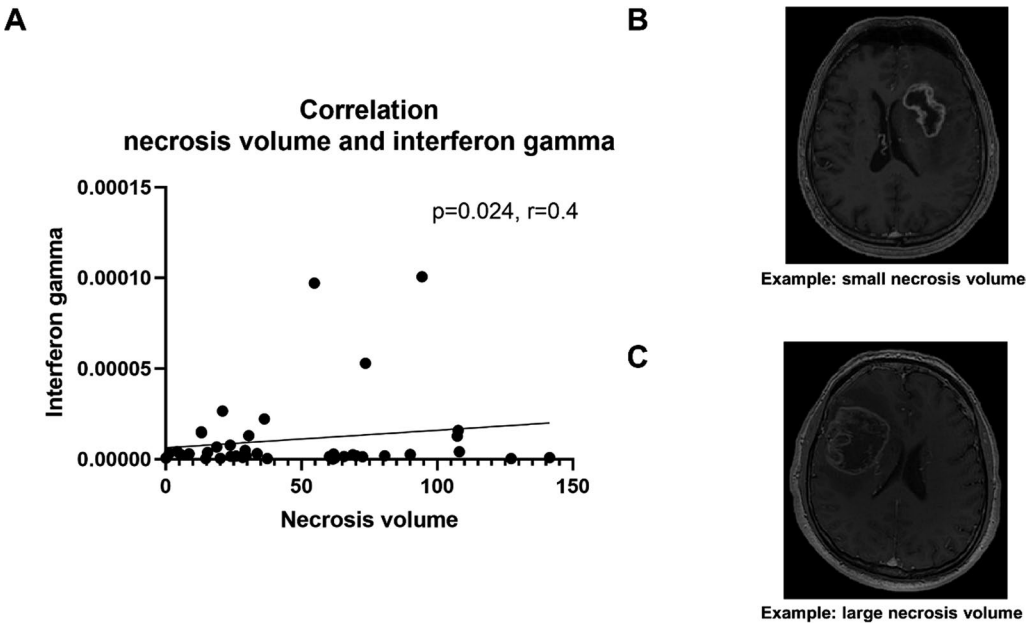

Fig. 4 Necrosis volume and interferon gamma in peripheral blood mononuclear cells. The necrosis volume correlated significantly with the abundance of interferon gamma mRNA in peripheral blood mononuclear cells (**a**). As illustration, an example of a patient with a relatively small necrosis volume (**b**) and a patient with a relatively large necrosis volume (**c**) are given. One value in the far upper right quadrant was removed for better readability of the chart, but was part of the calculation

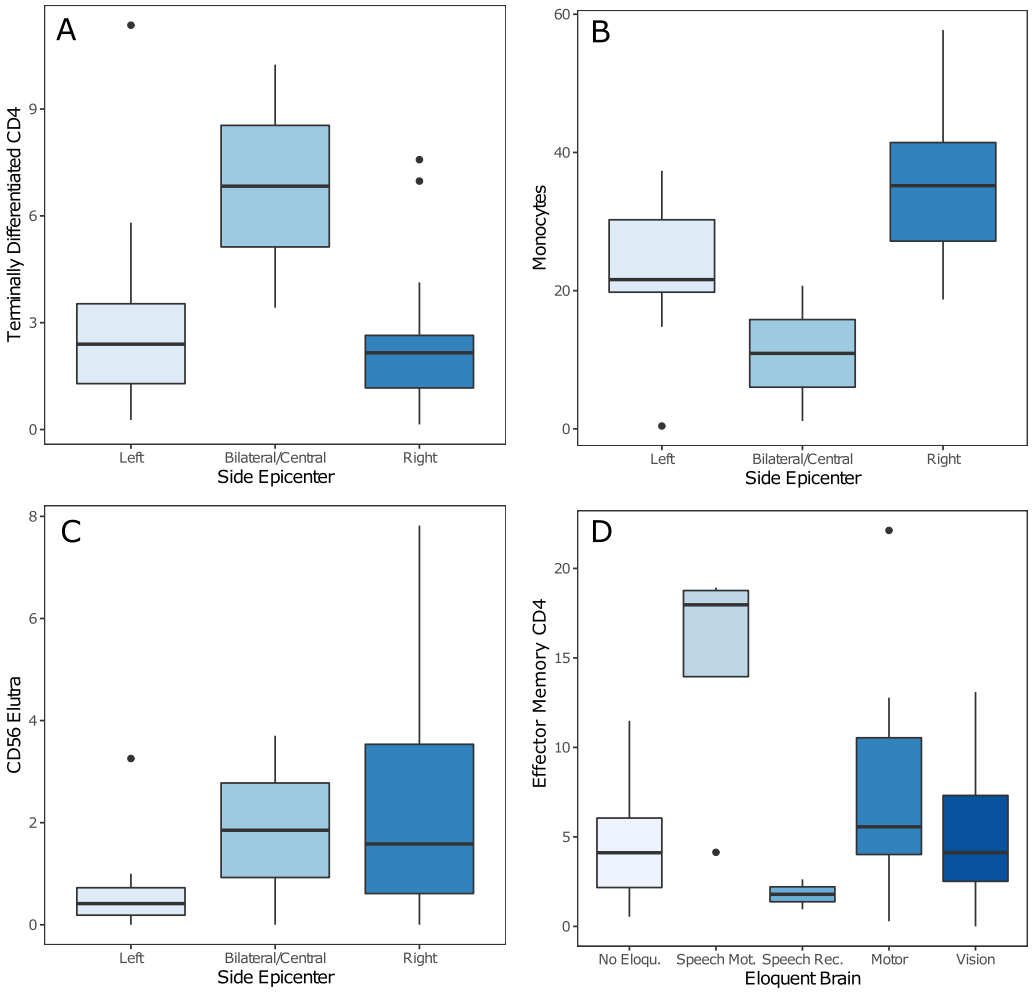

Fig. 5 Boxplots showing results of ANOVA analysis between categorical imaging and immunology variables. Bilateral/Central tumors had a significantly higher number of terminally differentiated CD4 cells (**a**). Tumors growing in the right hemisphere had a significantly higher number of monocytes (**b**), and a significantly higher number of CD56 cells (measured after elutriation, **c**). Tumors located in the speech motor area had the highest number of effector memory CD4 cells (**d**). no eloqu.: non-eloquent brain, speech mot.: speech motor, speech rec.: speech receptive

bilateral-right, $p=0.010$). (C) CD56+ NK cells in the blood were less abundant in left-sided tumors (left–right, $p=0.027$). (D) And effector memory CD4+ helper T cells in the blood were higher for tumors located in the Broca area than for tumors located in the Wernicke area ($p=0.024$) or non-eloquent brain regions ($p=0.04$).

Identification of most reliable imaging-immunology-associations via multiple testing correction

Next, we combined the initial broad screenings with multiple testing correction computations to identify the most reliable imaging-immunology-associations. In that strict, focused analysis, the hitherto described associations were narrowed down to two significant findings: The "thickness of the enhancing margin" was significantly negatively correlated with regulatory T cell markers in the peripheral blood ($p<0.0001$, $r=-0.3$, Fig. 6). Thus, the thicker the contrast-enhancing margin was, the less regulatory T cell factors were found in the blood. And, the circumstance of "deep white matter invasion" was significantly associated with the abundance of T helper 17 (Th17)-associated factors in the peripheral blood ($p=0.0002$, $r=-0.5$, Supplementary Fig. 2). Hence, in those cases where deep white matter structures like the corpus callosum or the internal capsule were invaded, the Th17 factors in the blood were significantly lower.

Automatic pattern detection via unsupervised data-driven techniques

Finally, after all the above-described investigations based on human-supervised statistical testing, we complemented our work with purely data-driven, unsupervised methods of pattern detection to look at the data from

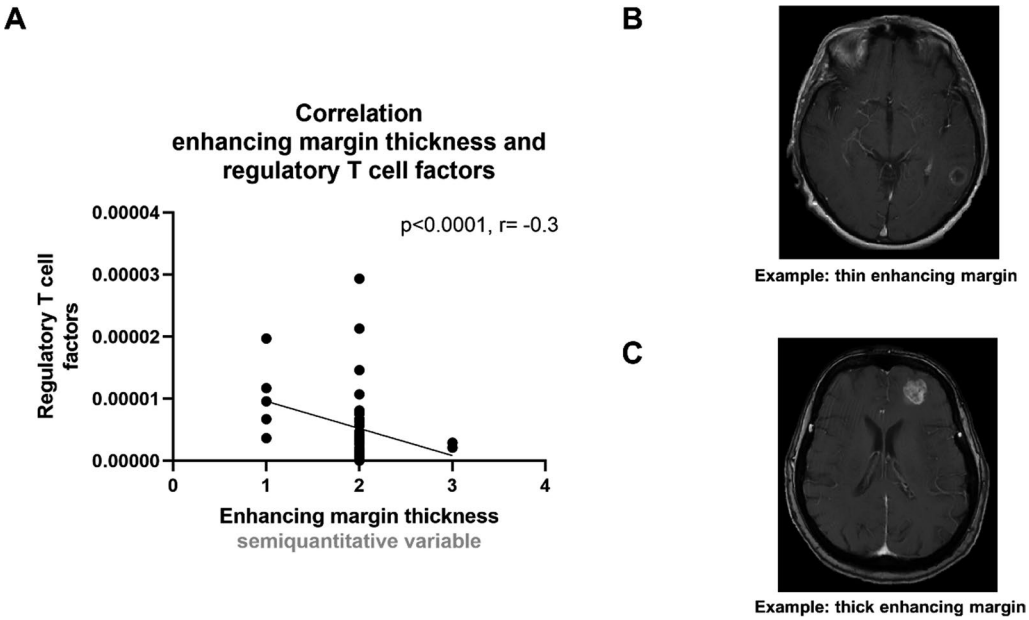

Fig. 6 Enhancing margin thickness and regulatory T cells transcription factors in the blood. The thickness of the enhancing margin (which is assessed semiquantitatively as an ordinal variable in the VASARI methodology: 1 = thin, 2 = thick, 3 = solid) correlated significantly with a lower abundance of regulatory T cells factors in the peripheral blood (**a**), as measured via Spearman correlation that is the adequate test for correlating semiquantitative/ordinal variables with quantitative variables. As illustration, an example of a patient with a relatively thin enhancing margin (**b**) and a patient with a relatively thick enhancing margin (**c**) are given - like in Fig. 3. Regulatory T cell factors here means a compund metric that integrates all measured regulatory T cell factors (i.e. IL-10, FoxP3, TGFbeta) to capture the concerted polarizing effect they have

yet another point of view. In that sense, a principal component analysis was performed (Supplementary Fig. 3). However, in this calculation no distinct principal components emerged. Similarly, we generated an unsupervised clustering heatmap that equally did not lead to unanimous variable clusters (Fig. 7). Likewise, the t-SNE algorithm did not arrive at a meaningful result (not shown). Thus, unsupervised methods did not yield additional insights at this point as no multidimensional patterns emerged.

Discussion

Main findings

In this study, we explored the interface between immunology and imaging in glioblastoma via mapping associations between peripheral blood immune system metrics and MRI morphological features of the tumor. We analysed an array of 27 radiological variables including the VASARI image description structure as well as 67 immunological variables stemming from blood flow cytometry and PCR. In an initial broad screening, we mapped numerous possible connections and morphological characteristics of the contrast-enhancing margin repeatedly showed up as immunology-related. Both, its thickness and its shape (i.e. the "definition": well-defined or poorly-defined), were positively correlated to pro-inflammatory immune variables: e.g. central memory CD8+ T cells were related to its thickness and e.g. activated CD8+ cytotoxic T cells, CD3+ T cells overall and CD56+ NK cells were related to its shape ("definition"). Apart from findings relating to the margin, the T2/FLAIR hyperintense T2 volume was e.g. correlated with CD56+CD16− NK cells in the blood. Finally, the necrosis volume was correlated with several immunostimulatory and immune-polarizing factors, i.e. IFN-γ (T helper 1 promoting), GATA3 (T helper 2 promoting) and RORgt (T helper 17 promoting). In an analysis of categorical variables, curiously, tumor location emerged as a potential predictor of immunophenotypes as e.g. certain CD4+ helper T cell types were more frequent in patients with central/bilateral tumors and in patients with tumors in the Broca area. As complementary analysis to the initial broad screening that was intended to give a full picture of potential imaging-immunology-associations, a strict multiple testing correction was performed as final step. Seen from that angle, the enhancing margin again showed up as its thickness was significantly correlated with lower regulatory T cells factors in the blood. Additionally, white matter invasion indicated significantly lower T helper 17 factors.

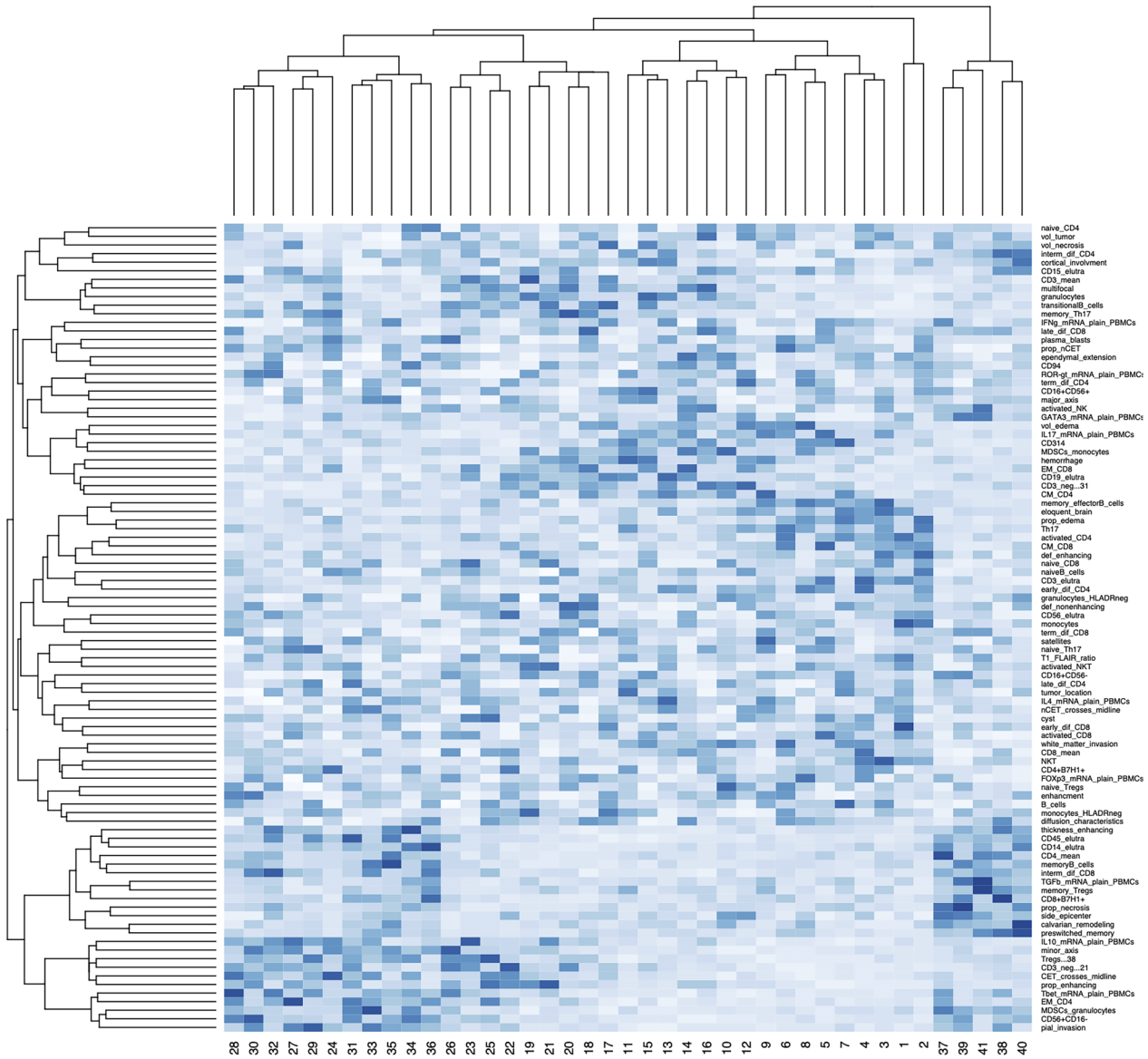

Fig. 7 Unsupervised data-driven techniques, exemplified by the k-means clustering heatmap shown here

Interpretation and prior literature

While others have integrated tumor morphology features with local tumor immunology [13], we seem to be the first to combine tumor analysis with systemic, i.e. peripheral blood, immunology.

Importantly, an analysis of connections between imaging features and survival measures was deliberately not in the scope of this study. In part, this question has already been dealt with in a prior publication [10] and in part it is not reasonable to conduct survival analyses based on the imaging-immunology findings made. Because we here exclusively concentrated on whether imaging characteristics can predict systemic immune states at baseline, all study participants were examined together, irrespectively if they had then later on received the immunotherapy or the standard-of-care therapy.

When evaluating the most eminent radiological feature findings (contrast-enhancing margin, T2 volume and necrosis volume) from an immunobiological point of view, their immunology connections seem to be plausible. Regarding the contrast-enhancing margin, it can be stated that the frontier of glioblastoma growth is apparently connected to the ongoing immune reaction that takes place where the blood–brain-barrier is likely disrupted. Here, it is fitting that various immune cells with cytotoxic, anti-tumor properties were found (e.g. CD8+

T cells, activated CD8+ T cells, central memory CD8+ T cells), which might reflect the body's efforts to reign in the tumor. Importantly, a thick enhancing margin was also correlated with lower regulatory T cell markers in the blood after multiple testing correction, again confirming that the enhancing margin relates to a systemic pro-inflammatory state. Similarly, the T2 hyperintense volume around a mass lesion in the brain is typically considered to be an expression of an ongoing immune reaction. This is also illustrated by the frequent usage of the immunosuppressant dexamethasone to control and reduce edema size in case of it being space-occupying and causing clinical symptoms [4]. That specific immune populations like CD56+CD16− NK cells and central memory CD8+ T cells in the blood are associated with it is, however, a novel observation. CD56+CD16− NK cells are often considered immune-regulatory [23] while central memory CD8+ T cells seem to be potent anti-tumoral cells and promising immunotherapy candidates as they can self-renew and give rise to cytotoxic effector cells leading to multiple rounds of attack against malignant cells [8]. One could deduct that opposing immunological forces are at play in the tumor edema and this is reflected in the blood. And, ultimately, the fact that different immunostimulatory and immune-polarizing transcription factors were associated with the necrosis volume might indicate the impact of immunogenic tumor cell death and release of damage-associated molecular patterns (DAMPs) caused by the necrosis [12]. All in all, the observations made and the apparent immune-imaging connections likely represent biologically reasonable insights. The most impactful finding is certainly that a thick enhancing margin represents a pro-inflammatory immune system state. Thus, we succeeded in establishing the argument for further venturing into the intersection of imaging and immunology in neurooncology. That tumor location seemed associated with specific immunophenotypes might be related to differences in blood perfusion of central versus distal brain regions or between eloquent and non-eloquent areas. At present, this is, however, purely speculative.

Potential clinical utility

One could imagine that systemic, blood-based immunophenotypes can in the future be defined based on imaging parameters. It could be truly helpful clinically and scientifically to estimate the current state of the immune system simply based on imaging. This would represent a versatile and practical approach for research and patient management. E.g. after additional confirmatory studies, it could be established that a thick enhancing margin reliably indicates lower regulatory T cell factors in the blood and thus a favourable anti-tumor immune state that might be a more amenable starting point for immunotherapy development. Hence, image features could potentially serve as biomarkers for (immuno)therapy research, application and selection.

Study limitations and future directions

This exploratory study—that aimed at providing a first mapping of imaging and immunology connections—comes with certain limitations. Obviously, the sample size is limited and the number of tested variables is substantial, leading to important multiple testing considerations. We purposefully started with a broad screening of all possible connections in order to first arrive at a comprehensive array of potentially useful findings and hypotheses. Then, we complemented this screening with an identification of the most reliable imaging-immunology connections via multiple testing correction. This way, we combined both analysis angles and present a thorough workup of the dataset in full breadth and depth. Additionally, further statistical computations were performed to confirm the validity of the findings. First, in order to validate VASARI feature correctness, we had two different VASARI assessors that independently analysed the images and we calculated the resulting inter-observer reliability, which was excellent ($\mathfrak{K} = 0.925$). Second, a retrospective power analysis with a sample size of 76 and a significance level of 0.05 was done for the correlation analysis and the one-way ANOVA tests. The achieved power was greater than 85%, indicating that the study has sufficient power to detect a significant effect. In Supplementary Tables 2 and 3 the calculated power for each individual test is given. Other than that, the segmentation of edema volume also has room for interpretation. We used a semi-automated active contour method (ITK-SNAP), which demonstrated excellent reliability and high efficiency of 3D segmentation in various previous projects from our group for tumor volumetry [10, 14, 26]. Thus, with this track record, we deem the used segmentation method as sufficiently reliable. But of course, all volumetry methods still have limitations that have to be taken into account when interpreting the findings. Finally, many observations we made seem to make sense biologically, which underlines their legitimacy. Taken together, various statistical and non-statistical considerations corroborate the validity of the findings made here. But nevertheless, we still regard them as a first exploration that will have to be confirmed by others.

The next caveat is that imaging and blood harvest were both at baseline of the study and thus in close temporal proximity, but not on exactly the same date—with blood harvest several days after imaging. However, the goal of this project was to capture stable immunological states

driven by lasting conditioning of the immune system through the tumor. Also, the order of interventions was the same for all patients. Therewith, we even see this temporal sequence as desirable because it corroborates that we identified major, steady immune phenotypes and it is compatible with real-word applications. Of note, the vast majority of immunological variables (62/67, 93%) were measured before brain tumor excision surgery. The only minor exception are the 5 immunological variables measured during the cell therapy production process (i.e. "elutriation" as a form of cell separation)—thus after surgery. If surgery had any effect, it could not have introduced a relevant bias as only a minimal fraction of the variables (5/67, 7%) was measured after it. And, these 5 "elutra" variables were not even the ones found as significantly relevant in this study. Any potential surgery bias introduced into the findings of this study can thus be excluded. But even if any of the 5 "elutra" variables would have been part of the main findings, a negative effect of surgery is questionable as in real-world settings the goal is to predict even post-surgical immune states from baseline, pre-surgery imaging, where e.g. the contrast-enhancing margin is still present.

Finally, another limitation is that so far we only used volumetry and the VASARI morphometry system but did not harness the potential of even more advanced imaging characterization like radiomics. Continuative studies could move into that direction. Likewise, what we could not consider in this study yet is the specific tissue genotype and tissue phenotype of the tumor itself—e.g. the microenvironment in terms of peritumoral neuropil infiltration and local immune states [5, 27, 30]. While in this study we had explicitly focused on the peripheral, systemic immune system, an integration of peripheral immunology and tumor-specific immunology (linked to neuropil infiltration patterns) would of course be desirable and shall be pursued in subsequent research.

Conclusion

With the analysis performed here, we pioneer the integration of imaging and systemic immunology in glioblastoma. Through the mapping of peripheral blood immune system metrics to MRI data we provide a reasonable starting point for future research and illustrate the usefulness of such an endeavour. Also, we provide first data on imaging-based immunophenotypes and add novel insights to basic glioblastoma immunobiology. The contrast-enhancing margin seems to be of particular prominence in that matter.

Supplementary Information

The online version contains supplementary material available at https://doi.org/10.1186/s40478-024-01888-8.

Additional file1

Author contributions

Conceptualization: HJ, MN, EF, Methodology: HJ, EF, writing—review and editing: HJ, VC, BJ, MC, RK, FT, WG, IS, NM, EF, Data curation: VC, BJ, MC, RK, FT, WG, NM, EF, Project administration: NM, EF, Supervision: EF. All authors have read and agreed to the published version of the manuscript.

Funding

This work was supported by the Medical Scientific Fund of the Mayor of the City of Vienna (*Fonds des Bürgermeisters der Stadt Wien*), via a grant to EF (Number 19071) and by the *Herbert Tumpel Preis* 2021 that was awarded to EF.

Availability of data and materials

The datasets used and/or analysed during the current study are available from the corresponding author on reasonable request.

Declarations

Ethics approval and consent to participate

The study had been reviewed and approved by the local independent ethics committee and institutional review board (Number TRX 2/P-II-018).

Consent for publication

All images depicted in this manuscript are entirely unidentifiable and there are no details on individual patients reported within the manuscript. Hence no consent for publication of individual human participants was required.

Competing interests

H.J.: None, V.C.: None, B.J.: None, M.C.: None, R.K.: None, F.T.: None, W.G.: Advisory Board Servier, I.S.: None, N.M.: None, E.F.: None.

Author details

[1]Department of Neurology, Medical University of Innsbruck, Innsbruck, Austria. [2]AOP Orphan Pharmaceuticals GmbH, Vienna, Austria. [3]University Clinic for Neurosurgery, Kepler University Hospital, Johannes Kepler University, Linz, Austria. [4]Clinical Division of Medical Oncology, Department for Internal Medicine I, Medical University of Vienna, Vienna, Austria. [5]Department of Neurosurgery, Medical University of Vienna, Vienna, Austria. [6]Independent Researcher, Vienna, Austria.

Received: 30 August 2024 Accepted: 10 November 2024
Published online: 27 November 2024

References

1. Azizova A, Prysiazhniuk Y, Wamelink I, Petr J, Barkhof F, Keil VC (2024) Ten years of VASARI glioma features: systematic review and meta-analysis of their impact and performance. AJNR Am J Neuroradiol 45:1053–1062. https://doi.org/10.3174/ajnr.A8274
2. Berger TG, Strasser E, Smith R, Carste C, Schuler-Thurner B, Kaempgen E, Schuler G (2005) Efficient elutriation of monocytes within a closed system (Elutra) for clinical-scale generation of dendritic cells. J Immunol Methods 298:61–72. https://doi.org/10.1016/j.jim.2005.01.005
3. Buchroithner J, Erhart F, Pichler J, Widhalm G, Preusser M, Stockhammer G, Nowosielski M, Iglseder S, Freyschlag CF, Oberndorfer S, Bordihn K, von Campe G, Hoffermann M, Ruckser R, Rössler K, Spiegl-Kreinecker S, Fischer MB, Czech T, Visus C, Krumpl G, Felzmann T, Marosi C (2018) Audencel

immunotherapy based on dendritic cells has no effect on overall and progression-free survival in newly diagnosed glioblastoma: a Phase II randomized trial. Cancers (Basel). https://doi.org/10.3390/cancers10100372
4. Cenciarini M, Valentino M, Belia S, Sforna L, Rosa P, Ronchetti S, D'Adamo MC, Pessia M (2019) Dexamethasone in glioblastoma multiforme therapy: mechanisms and controversies. Front Mol Neurosci 12:65. https://doi.org/10.3389/fnmol.2019.00065
5. De Fazio E, Pittarello M, Gans A, Ghosh B, Slika H, Alimonti P, Tyler B (2024) Intrinsic and microenvironmental drivers of glioblastoma invasion. Int J Mol Sci 25:1. https://doi.org/10.3390/ijms25052563
6. Di Ianni N, Maffezzini M, Eoli M, Pellegatta S (2021) Revisiting the immunological aspects of temozolomide considering the genetic landscape and the immune microenvironment composition of glioblastoma. Front Oncol 11:747690. https://doi.org/10.3389/fonc.2021.747690
7. Erhart F, Buchroithner J, Reitermaier R, Fischhuber K, Klingenbrunner S, Sloma I, Hibsh D, Kozol R, Efroni S, Ricken G, Wöhrer A, Haberler C, Hainfellner J, Krumpl G, Felzmann T, Dohnal AM, Marosi C, Visus C (2018) Immunological analysis of phase II glioblastoma dendritic cell vaccine (Audencel) trial: immune system characteristics influence outcome and Audencel up-regulates Th1-related immunovariables. Acta Neuropathol Commun 6:135. https://doi.org/10.1186/s40478-018-0621-2
8. Gehad A, Teague JE, Matos TR, Huang V, Yang C, Watanabe R, O'Malley JT, Trimble CL, Kupper TS, Clark RA (2018) A primary role for human central memory cells in tissue immunosurveillance. Blood Adv 2:292–298. https://doi.org/10.1182/bloodadvances.2017011346
9. Gu Z (2022) Complex heatmap visualization. iMeta 1:e43. https://doi.org/10.1002/imt2.43
10. Heugenhauser J, Galijasevic M, Mangesius S, Goebel G, Buchroithner J, Erhart F, Pichler J, Widhalm G, Stockhammer G, Iglseder S, Freyschlag CF, Oberndorfer S, Bordihn K, von Campe G, Czech T, Surböck B, Urbanic Purkart T, Marosi C, Felzmann T, Nowosielski M (2022) MRI response assessment in glioblastoma patients treated with dendritic-cell-based immunotherapy. Cancers (Basel). https://doi.org/10.3390/cancers14061579
11. Horikoshi M, Tang Y (2016) ggfortify: data visualization tools for statistical analysis results
12. Hou J, Han ZP, Jing YY, Yang X, Zhang SS, Sun K, Hao C, Meng Y, Yu FH, Liu XQ, Shi YF, Wu MC, Zhang L, Wei LX (2013) Autophagy prevents irradiation injury and maintains stemness through decreasing ROS generation in mesenchymal stem cells. Cell Death Dis 4:e844. https://doi.org/10.1038/cddis.2013.338
13. Hsu JB, Lee GA, Chang TH, Huang SW, Le NQK, Chen YC, Kuo DP, Li YT, Chen CY (2020) Radiomic immunophenotyping of GSEA-assessed immunophenotypes of glioblastoma and its implications for prognosis: a feasibility study. Cancers (Basel). https://doi.org/10.3390/cancers12103039
14. Iglseder S, Iglseder A, Beliveau V, Heugenhauser J, Gizewski ER, Kerschbaumer J, Stockhammer G, Uprimny C, Virgolini I, Dudas J, Nevinny-Stickel M, Nowosielski M, Scherfler C (2023) Somatostatin receptor subtype expression and radiomics from DWI-MRI represent SUV of [68Ga]Ga-DOTATOC PET in patients with meningioma. J Neurooncol 164:711–720. https://doi.org/10.1007/s11060-023-04414-3
15. Jackson CM, Choi J, Lim M (2019) Mechanisms of immunotherapy resistance: lessons from glioblastoma. Nat Immunol 20:1100–1109. https://doi.org/10.1038/s41590-019-0433-y
16. Jarosz Q (2020) VASARI research project. https://wiki.cancerimagingarchive.net/display/Public/VASARI+Research+Project. Accessed 26 April 2023
17. Karachi A, Dastmalchi F, Mitchell DA, Rahman M (2018) Temozolomide for immunomodulation in the treatment of glioblastoma. Neuro Oncol 20:1566–1572. https://doi.org/10.1093/neuonc/noy072
18. Krijthe J, Van der Maaten L (2023) Rtsne: T-distributed stochastic neighbor embedding using a Barnes–Hut implementation. https://cran.r-project.org/web/packages/Rtsne/index.html.
19. Lapa C, Linsenmann T, Lückerath K, Samnick S, Herrmann K, Stoffer C, Ernestus RI, Buck AK, Löhr M, Monoranu CM (2015) Tumor-associated macrophages in glioblastoma multiforme—a suitable target for somatostatin receptor-based imaging and therapy? PLoS ONE 10:e0122269. https://doi.org/10.1371/journal.pone.0122269
20. Lim M, Xia Y, Bettegowda C, Weller M (2018) Current state of immunotherapy for glioblastoma. Nat Rev Clin Oncol 15:422–442. https://doi.org/10.1038/s41571-018-0003-5
21. Louis DN, Perry A, Reifenberger G, von Deimling A, Figarella-Branger D, Cavenee WK, Ohgaki H, Wiestler OD, Kleihues P, Ellison DW (2016) The 2016 World Health Organization classification of tumors of the central nervous system: a summary. Acta Neuropathol 131:803–820. https://doi.org/10.1007/s00401-016-1545-1
22. Meier R, Pahud de Mortanges A, Wiest R, Knecht U (2020) Exploratory analysis of qualitative MR imaging features for the differentiation of glioblastoma and brain metastases. Front Oncol 10:581037. https://doi.org/10.3389/fonc.2020.581037
23. Michel T, Poli A, Cuapio A, Briquemont B, Iserentant G, Ollert M, Zimmer J (2016) Human CD56bright NK cells: an update. J Immunol 196:2923–2931. https://doi.org/10.4049/jimmunol.1502570
24. Morimura T, Neuchrist C, Kitz K, Budka H, Scheiner O, Kraft D, Lassmann H (1990) Monocyte subpopulations in human gliomas: expression of Fc and complement receptors and correlation with tumor proliferation. Acta Neuropathol 80:287–294. https://doi.org/10.1007/bf00294647
25. Nesseler JP, Schaue D, McBride WH, Lee MH, Kaprealian T, Niclou SP, Nickers P (2019) Irradiation to improve the response to immunotherapeutic agents in glioblastomas. Adv Radiat Oncol 4:268–282. https://doi.org/10.1016/j.adro.2018.11.005
26. Nowosielski M, Goebel G, Iglseder S, Steiger R, Ritter L, Stampfl D, Heugenhauser J, Kerschbaumer J, Gizewski ER, Freyschlag CF, Stockhammer G, Scherfler C (2022) ADC textural features in patients with single brain metastases improve clinical risk models. Clin Exp Metastasis. https://doi.org/10.1007/s10585-022-10160-z
27. Pombo Antunes AR, Scheyltjens I, Duerinck J, Neyns B, Movahedi K, Van Ginderachter JA (2020) Understanding the glioblastoma immune microenvironment as basis for the development of new immunotherapeutic strategies. Elife. https://doi.org/10.7554/eLife.52176
28. Pope WB, Sayre J, Perlina A, Villablanca JP, Mischel PS, Cloughesy TF (2005) MR imaging correlates of survival in patients with high-grade gliomas. AJNR Am J Neuroradiol 26:2466–2474
29. Schaff LR, Mellinghoff IK (2023) Glioblastoma and other primary brain malignancies in adults: a review. JAMA 329:574–587. https://doi.org/10.1001/jama.2023.0023
30. Seker-Polat F, Pinarbasi Degirmenci N, Solaroglu I, Bagci-Onder T (2022) Tumor cell infiltration into the brain in glioblastoma: from mechanisms to clinical perspectives. Cancers (Basel). https://doi.org/10.3390/cancers14020443
31. Tang Y, Horikoshi M, Li W (2016) ggfortify: unified interface to visualize statistical result of popular R packages. The R Journal 8:474. https://doi.org/10.32614/RJ-2016-060
32. van der Maaten L (2014) Accelerating t-SNE using tree-based algorithms. J Mach Learn Res 15:3221–3245
33. van der Maaten LJP, Hinton GE (2008) Visualizing high-dimensional data using t-SNE. J Mach Learn Res 9:2579–2605
34. Yushkevich PA, Piven J, Hazlett HC, Smith RG, Ho S, Gee JC, Gerig G (2006) User-guided 3D active contour segmentation of anatomical structures: significantly improved efficiency and reliability. Neuroimage 31:1116–1128. https://doi.org/10.1016/j.neuroimage.2006.01.015

Publisher's Note